Available online at www.sciencedirect.com
SCIENCE DIRECT®
Carbohydrate Polymers 55 (2004) 101–112
Carbohydrate Polymers
www.elsevier.com/locate/carbpol

Controlled γ-ray irradiation of heparin generates oligosaccharides enriched in highly sulfated sequences

Antonella Bisio[a], Sara Guglieri[a], Marta Frigerio[a], Giangiacomo Torri[a,*], Elena Vismara[b], Umberto Cornelli[c], Donata Bensi[d], Sergio Gonella[d], Luigi De Ambrosi[d]

[a]*Istituto di Ricerche Chimiche e Biochimiche G. Ronzoni, V.G. Colombo 81, 20133 Milan, Italy*
[b]*G. Natta Chemistry Department, Polytechnic of Milan, V. Mancinelli 7, 20131 Milan, Italy*
[c]*Department of Pharmacology, Loyola University Chicago, Stritch School of Medicine, 2160 South First Avenue, Maywood, IL 601533, USA*
[d]*Laboratori Derivati Organici, V.M. Barozzi 4, 20122 Milan, Italy*

Received 20 June 2003; accepted 18 August 2003

Abstract

Controlled physical depolymerization of heparin was performed in aqueous solution in the presence of isopropanol by γ-irradiation. Isopropanol both makes selective the radical-induced scission of the glycosidic linkage involved in the depolymerization and acts as hydrogen donor scavenger of heparin intermediate radicals that usually result in UV-absorbing by-products.

Several preparations of heparin-derived oligosaccharides (HDO) were reproducibly obtained from different unfractionated heparins (UFH). From each preparation, an intermediate fraction with an average molecular weight of about 2200 Da (γ-HDO) was isolated by gel permeation chromatography and its sulfation pattern was characterized by nuclear magnetic resonance spectroscopy. The comparison of the sulfation pattern of HDO with that of parent UFHs revealed a significant decrease in the relative content of D-glucuronic acid with respect to the total amount of uronic acid.

Further γ-ray treatments of heparin chains that survived the first depolymerization procedure led to a further decrease of D-glucuronic acid and also slightly reduced the content of *N*-acetyl-glucosamine residues, thus enriching oligosaccharide chains in the highly sulfated sequences. MALDI mass spectrometric analysis of oligomeric components indicated that γ-HDO prevalently contains highly sulfated chains (tetra to decasaccharides, including both odd and even number of monosaccharidic units) chiefly constituted of repeating sequences of the trisulfated disaccharide L-iduronic acid 2-sulfate (1 → 4) D-glucosamine-*N*,6 disulphate.

γ-Irradiation in the presence of isopropanol thus generated heparin fragments largely preserving the prevalent structure of the parent heparin and involved glucuronic acid as the major site of cleavage.

Keywords: Heparin oligosaccharides; γ-Irradiation; Scavenger; Sulfation pattern; Nuclear magnetic resonance; MALDI-TOF

1. Introduction

Heparin is a heterogeneous, polydisperse, highly sulfated polysaccharide belonging to the family of glycosaminoglycans, made up of 1 → 4 linked disaccharide repeating units, consisting of an α-D-glucosamine (A) and a hexuronic acid, α-L-iduronic (I) or β-D-glucuronic (G) acid, with *O*-sulfate groups at different positions of the disaccharide unit, especially at position 2 of the iduronic (I_{2S}) and positions 3 and 6 of the glucosamine (A_{3S}, A_{6S}), and *N*-sulfate or *N*-acetyl groups at position 2 of the glucosamine residue (A_{NS}, A_{NAc}). The most frequently occurring repeating disaccharide sequence is → 4)-α-L-iduronic acid-2-*O*-sulfate-(1 → 4)-α-D-glucosamine-*N*,6-disulfate (1 → (I_{2S}–$A_{NS,6S}$), which represents the heparin highly sulfated segment, located closer to the non-reducing terminal of the heparin chain. Undersulfated sequences, accounted for by non-sulfated I and G, and A_{NAc} are prevalently located toward the reducing end of the polymer. About one-third of heparin chains contains a specific pentasaccharidic sequence, characterized by a central $A_{NS,6S}$ residue bearing an extra sulfate group at position 3 ($A_{NS,3S,6S}$), constituting the active site for antithrombin III (AT). Many biochemical

* Corresponding author. Tel.: +39-02-7064-1621; fax: +39-02-7064-1634.
E-mail address: torri@ronzoni.it (G. Torri).

0144-8617/$ - see front matter © 2004 Elsevier Ltd. All rights reserved.
doi:10.1016/j.carbpol.2003.08.017

models as well as structural studies suggest that such pentasaccharide is located between the highly and the undersulfated domains (Casu, 1985; Dietrich et al., 1998; Lindahl, Kusche-Gulberg, & Kjellen, 1998; Petitou et al., 2001). A minor sequence, involving neutral residues as galactose and xylose and corresponding to the reducing end of the polysaccharide chain, is the linkage region (LR) to the core protein of the original proteoglycan.

The large number of possible structural variants of heparin sequences accounts for the wide range of biological activities that heparin promotes by binding to different plasma and tissue proteins, such as protease inhibitors of blood coagulation cascade, growth factors, chemokines, adhesive matrix proteins, etc. (Capila & Linhardt, 2002). The identification of specific heparin structures responsible for binding to various protein ligands is of increasing interest. While some proteins, as AT, have affinity only for unique irregularities of heparin structure, others recognize the most regular regions of heparin, though this fact does not exclude selectivity of binding (Maccarana, Casu, & Lindahl, 1993).

Depending on their size and structural arrangement, heparin-derived oligosaccharides (HDO) may elicit or inhibit specific biological effects (Casu & Lindahl, 2001; Gambarini, Miyamoto, Lima, Nader, & Dietrich, 1993; Moy et al., 1997; Sudhalter, Folkman, Svahn, Bergendal, & D'Amore 1989). Typically, heparin sequences with a length ranging from tetra to decasaccharides are responsible for modulation of biological activity of proteins (Venkataraman, Shriver, Raman, & Sasisekharan, 1999a). Different low and ultra-low molecular weight heparin derivatives, ranging from 1900 to 4600 Da, were recently demonstrated to cross the blood-brain barrier (BBB) in rats after oral or intravenous administration and to exert a neuroprotective effect, potentially exploitable in the therapeutic treatment of neurodegenerative disorders (Leveugle et al., 1998; Rose, Dudas, Cornelli, & Hanin, 2003; Walzer et al., 2002). It is currently unclear what molecular weight fraction of these heterogeneous compounds crosses the BBB, and also what structural requirement is related to the biological action in the brain. The structural heterogeneity of heparin greatly influences the structure of the corresponding oligosaccharides. Moreover, each depolymerization reaction used for their preparation presents its own preferential selectivity, with respect to sequences and/or residues, and also usually modify at least the monosaccharide at the site of cleavage, generating further structural diversities (Casu & Torri, 1999).

In the present work we have exploited a controlled physical depolymerization process with γ-rays, to obtain oligosaccharides from pig mucosal heparin (γ-HDO) (Gonella, De Ambrosi, & Vismara, 2002). That approach could be promising as the most conspicuous result of the γ-irradiation of polysaccharides in solution was depolymerization (Von Sonntag, Dizdaroglu, & Schulte-Frohlinde, 1976). Heparin depolymerization by γ-irradiation is thought to occur via mechanisms of radical-induced scission of the glycosidic linkage (Fig. 1). This work describes a γ-ray process for the depolymerization of heparin in the presence of isopropanol, selected from ethers, alcohols, esters and carboxylic acids, which have been proposed as modulators of the radical mechanisms involved and as hydrogen donor radical scavenger of heparin radical intermediate adducts. The work also involved the structural characterization of heparin oligosaccharides obtained by this process.

Four preparations of γ-HDO were isolated and characterized by nuclear magnetic resonance spectroscopy (NMR) and their sulfation pattern was compared with that of several unfractionated heparins (UFHs) including the parent heparins. Moreover, in order to study the effect of γ-ray treatment on heparin structure, in a single case, the heparin chains that survived the depolymerizing reaction were recovered by gel chromatography and further γ-irradiated. This procedure was repeated twice. All the products obtained have been structurally characterized and compared with parent UFHs also in terms of molecular weight distribution and anticoagulant (antifactor Xa) activity in vitro. In addition, MALDI MS analysis of γ-HDO preparation provided an assessment of the main oligosaccharidic components.

2. Experimental

Materials. Pig mucosal heparins were commercial preparations of unfractionated sodium salt heparin (UFH) from Laboratori Derivati Organici. Sephadex G50 was obtained from Amersham Pharmacia Biotech, Uppsala, Sweden. TSK columns were from Supelco, Bellefonte, PA, USA. Human antithrombin, bovine factor Xa and synthetic substrate S-2765 were from Chromogenix (Mölndal, Sweden). All other reagents and chemicals were of research grade.

Identification of a modulator suitable for the depolymerization reaction. A series of alcohols, ethers, and esters (isopropanol, ethanol, tetrahydrofuran, glyoxal trimeric dihydrate, formic acid, acetic acid, dimethylmalonate) were tested. Eight 10% (w/v) aqueous heparin solutions were prepared, seven containing each one an organic compound among the above-mentioned, in 0.1 M concentration, and the eighth one with nothing else. They were subjected to a total amount of radiation of 180 kGy. On each depolymerized mixture, the average molecular weight and the absorbance at 260 and 400 nm were evaluated. Absorbance at 260 and 400 nm was determined by diluting the samples according to European Pharmacopoeia 4th ed 01/2002:0828 p. 1297.

Identification of the isopropanol concentration for the depolymerization reaction. Further experiments were carried out to find the proper concentration of isopropanol in the reaction media using three different molarities.

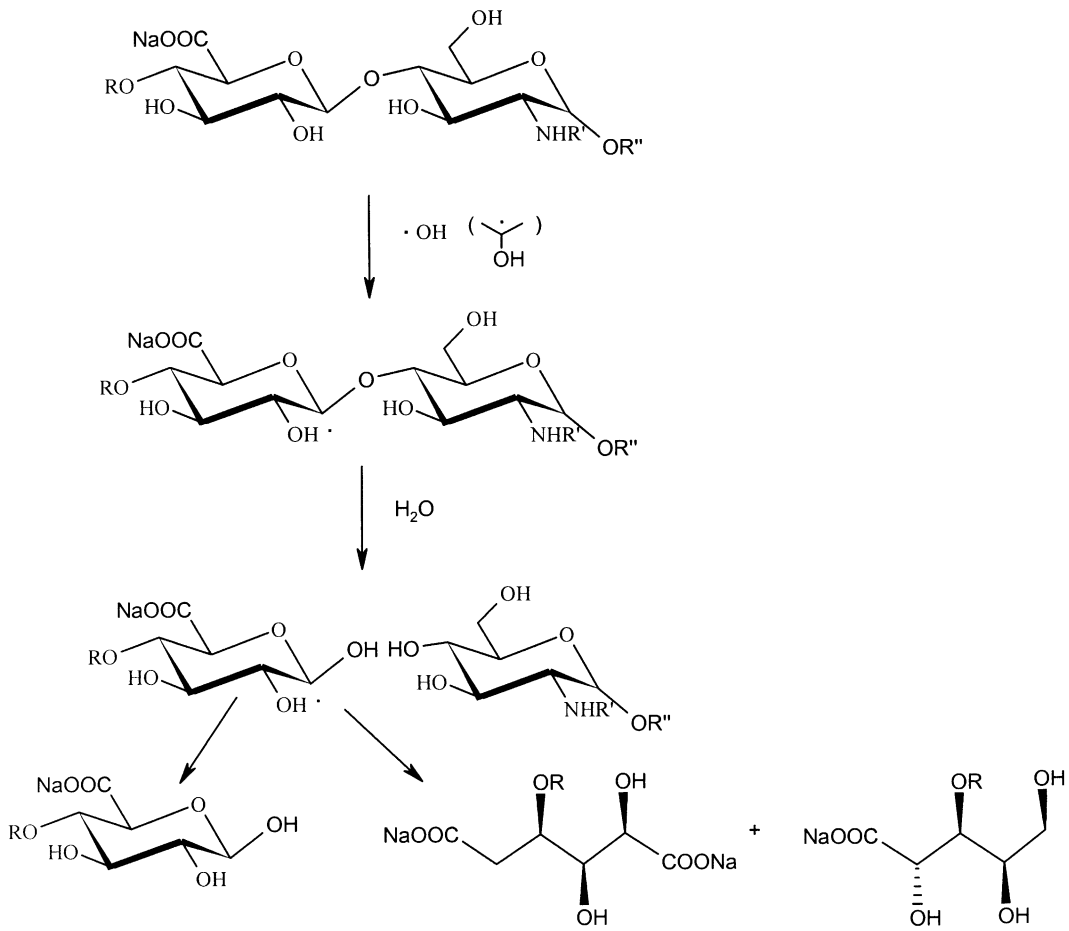

Fig. 1. Mechanisms of radical-induced scission of glycosidic linkage proposed for γ-irradiated heparin.

HDO preparation. An aqueous solution of pig mucosal heparin (10% w/v), in the presence of 0.4% (v/v) isopropanol and under nitrogen atmosphere, was submitted to ionizing radiation (180–200 kGy) using ^{60}Co as gamma emitter, according to well-defined and controlled physical parameters (Gonella et al., 2002). The depolymerized heparin mixture was subjected to a bleaching treatment with oxidizing agents, according to typical industrial procedures for heparin preparations. A single preparation (γ-HDOa) was studied in more detail; it was applied to a Sephadex G50 gel permeation column in order to separate higher (H) and lower (L) molecular weight species and isolate an intermediate fraction (γ-HDO). Fraction H, separated from γ-HDOa was recovered and re-submitted to γ-ray treatment followed by gel chromatographic fractionation under the same conditions as above, obtaining fractions H2, HDOa2 and L2. Then, fraction H2 was once again treated with γ-rays and fractionated as above, producing fractions H3, HDO-a3 and L3. Total recovery of the three γ-HDO fractions (a, a2 and a3) was about 35%.

Determination of molecular weight. The average molecular weights and molecular weight distributions of HDO preparations were determined by using two high performance gel permeation chromatography columns, TSK G2000 and TSK G3000 (7.5 × 300 mm^2) and a guard column SW (7.5 × 7.5 mm^2) connected in series. Samples were dissolved in the mobile phase (0.2 mol/l sodium sulfate pH 5) at a concentration of 10 mg/ml. Elution was performed at a flow rate of 0.5 ml/min and effluents were monitored by measuring the absorbance at 234 nm.

Biological activity. The in vitro anti-Xa activity, expressing inhibition of factor Xa by antithrombin, was determined using an amidolytic assay according to the European Pharmacopoeia (3rd edition, 1997:0828) specifications (Teien & Lie, 1977). Human antithrombin, bovine factor Xa and synthetic substrate S2765 were from Chromogenix (Mölndal, Sweden).

NMR spectra. The proton spectra were obtained with 500 MHz on a Bruker Avance spectrometer, equipped with gradient TXI 5 mm probe, at 60 °C, with presaturation of the residual water signals, recycle delay of 12 s and number of scans 128. Samples were prepared by dissolving10 mg of γ-HDO or UFH in 0.5 ml of deuterium oxide (99.99%). The ^{1}H/^{13}C chemical shift correlation (HSQC) spectra were performed using z-gradients for coherence selection. They were obtained with carbon decoupling during acquisition period in phase sensitivity-enhanced pure absorption mode. The spectra were acquired with a nulling time of 2 s, 1024

data points in F2, 512 increments in F1, and 32 scans per increment. The final matrix size was zero-filled to 4K × 2K and multiplied with shifted (π/3) sine-bell-square prior Fourier transformation. Integration of cross-peak volumes was performed using Bruker XWINNMR 3.1 software package.

The carbon spectra were obtained at 100 MHz on a Bruker AMX400 spectrometer equipped with broadband 10 mm probe at 40 °C. Protons were decoupled during the acquisition time. Recycle delay was 4 s and the number of scans 40,000. Samples were prepared by dissolving 250 mg of UFH or γ-HDO in 2.5 ml of deuterium oxide.

Quantification of sulfation patterns. The percentage of all the possible substituents present on glucosamine or uronic acid rings were referred to the total area of glucosamine and uronic acid ^{1}H NMR signals, respectively, and calculated as previously described (Guerrini, Bisio, & Torri, 2001). In addition, the content of reducing 2-*O*-sulfated iduronic acid residues was calculated. Since H1 signal of I_{2S} only accounts for the 1 → 4 linked residues, the percentage of the I_{2S} at the reducing end was determined from the ^{13}C NMR spectra: the signal at 95 ppm was integrated, compared to 1/2 of the area of anomeric signals, and the resulting percentage was taken in account for the calculation of the amount of I_{2S} obtained from proton spectra. Moreover, the percentage of total *N*-sulfated glucosamine (A_{NS}) residues, calculated by integration of the H2 signal at 3.3 ppm, was split into A_{NS} linked to iduronic acid (A_{NS}-I) and A_{NS} linked to glucuronic acid (A_{NS}–G)(20). The latter was quantified by integrating its anomeric proton signal, at 5.6 ppm, while A_{NS}–I was determined by the difference between total A_{NS} and the H1 of A_{NS}–G.

Charge fractionation of γ-HDO. 500 mg of γ-HDOc preparation dissolved in equilibrating solution, NH_4Cl 0.05 M pH 7.4, were loaded on QAE-Sephadex A25-120 column (2.5 × 5 cm^2) and fractionated into four fractions by eluting with a stepwise increasing concentration of NaCl (0.4, 0.8, 1.0 and 2.0 M) in 60 ml of equilibrating solution, at a flow rate of 0.8 ml/min. The corresponding fractions, γ-HDOc-0.4, γ-HDOc-0.8, γ-HDOc-1.0 and γ-HDOc-2.0, were desalted by gel permeation chromatography on Sephadex G10 and analysed for uronic acid content by carbazole reaction (Bitter & Muir, 1962): their yields were 15, 61, 23 and 1%, respectively.

MALDI mass spectrometry. MALDI analyses were carried out in the positive ion linear mode on a Bruker Biflex III time-of-flight mass spectrometer (Bruker Saxonia Analytik, GmbH, Leipzig, Germany) equipped with a pulse nitrogen laser (λ = 337 nm). A matrix solution (caffeic acid 12 mg/ml in 50% AcCN/H_2O) containing equimolar concentrations (2.5 pmol/μl) of basic peptide (Arg–Gly)$_{19}$–Arg (Sigma-Genosys Ltd, Cambridge, England) (as free base, after ionic exchange on a Dowex 1 × 2 resin) (Venkataraman, Shriver, Davis, & Sasisekharan, 1999b) was mixed with an aqueous solution of oligosaccharide fraction γ-HDOc0.8 at a molar ratio of 2:1. One microlitre of the final mixture was deposited on the stainless steel target of the spectrometer favouring sample crystallization at room temperature and atmospheric pressure. Mass spectra were calibrated externally with BSA and cytochrome c. MALDI acquisitions were performed by collecting and summing 'batches' of a few laser shots at a threshold laser power (Farmer & Caprioli, 1998). The final spectra are the result of average sampling at different crystal surface position.

3. Results

Table 1 reports MW and absorbance in UV/visible region of crude depolymerized heparins obtained from a set of experiments, run under the same irradiation conditions. Heparin was irradiated alone or in the presence of isopropanol, ethanol, tetrahydrofuran, glyoxal trimeric dihydrate, formic acid, acetic acid and dimethylmalonate. The table also reports the bond dissociation energies (BDE) for the selected molecules (George, El Rassy, & Chovelon, 2001). The lowest MW was obtained when heparin was irradiated alone, but the obtained product revealed very high absorbancy values at 260 and 400 nm (2.130 and 0.420, respectively), in comparison with the corresponding values found for starting heparin (0.047 and 0.006, respectively). Isopropanol, ethanol, tetrahydrofuran and glyoxal trimeric dihydrate favoured depolymerization (MW under 4000 Da) and at the same time isopropanol, ethanol and tetrahydrofuran significantly reduced the UV/visible absorbancies. In the presence of formic acid, acetic acid and dimethylmalonate the MW was higher than 4000 Da and only formic acid reduced the absorbancies. Since THF is very toxic and

Table 1
Molecular weight (MW) and absorbance in UV/visible region of heparin solutions depolymerized by γ-rays alone or in the presence of weak C–H bond organic compounds selected on the basis of the bond dissociation energy (BDE)

Organic compound	MW (Da)	Abs 400 nm	Abs 260 nm	BDE (kJ mol^{-1})[a]
None	3300	0.420	2.130	–
(after oxidizing treatment)	3300	0.110	0.616	
Isopropanol	3750	0.160	0.970	381
(after oxidizing treatment)	3750	0.024	0.285	
Ethanol	3600	0.120	0.930	389
Tetrahydrofuran	3900	0.100	0.790	385
Glyoxal	3500	0.290	1.030	387
Formic acid	4500	0.210	1.080	387
Acetic acid	4700	0.520	2.060	410
Dimethylmalonate	4200	0.440	1.940	444
γ-HDO	2200		0.180	

Values after oxidizing treatment are also reported. MW and UV absorbance values of a typical purified γ-HDO are indicated.
[a] Literature data (George et al., 2001).

Table 2
Molecular weight (MW), polydispersity (Pd) and in vitro anti-Xa potency of six preparations of γ-HDO, obtained with single (a–d), double (a2) and triple (a3) γ-ray treatment, in comparison with a typical UFH

Sample	MW (Da)	Pd	Anti-Xa activity (U/mg)
UFH	16,500	1.28	190
γ-HDO-a	2100	1.28	43
γ-HDO-b	2200	1.33	35
γ-HDO-c	2200	1.28	43
γ-HDO-d	2300	1.23	43
γ-HDO-a2	2000	1.30	35
γ-HDO-a3	2200	1.25	34

ethanol is not a good choice from an industrial point of view, isopropanol was utilized for the depolymerizations described below.

All the different γ-HDO analysed, prepared in the presence of isopropanol both with single (γ-HDOa–d) or additional (γ-HDOa2 and γ-HDOa3) γ-ray treatments, exhibited comparable and symmetrical HPLC elution profiles. Their molecular weight and polydispersity values are listed in Table 2, together with their resulting in vitro anticoagulant (anti-Xa) activity, in comparison with the corresponding values of a typical UFH. The mean values and the standard deviations of both molecular weight and anti-Xa potency are 2150 ± 94 Da and 39 ± 4 U/mg, respectively.

Typical ^{13}C and ^{1}H spectra of γ-HDO in comparison with the corresponding UFH sample are shown in Figs. 2 and 3, respectively. The profiles of oligosaccharide spectra are similar to that of parent heparin, with the differences typically induced by depolymerization, generally such as sharpening signal, because of reduced viscosity, and stronger resonances associated with chain terminals and sequence effects. For instance, the new signals at 93 and 95 ppm in the γ-HDO ^{13}C spectrum, are attributed to the anomeric carbons of the reducing *N*,6-sulfated glucosamine and 2-sulfated iduronic acid residues, respectively (Bisio et al., 2001).

From the comparison of proton spectra of γ-HDO and parent heparin some diversities appear. The main difference is due to the impressive increase of intensity of the signal of the H4 of the non-reducing *N*,6-sulfated glucosamine residue at 3.56 ppm (Bisio et al., 2001). Other differences are due to reducing end resides: for instance, H2 resonances at about 3.1 and 3.2 ppm of β anomers of A_{NS} and G, respectively, while H1 resonance at 5.44 ppm is of the α anomer of A_{NS}.

A method combining ^{1}H and ^{13}C quantitative analysis of major and some minor signals, originally set-up for UFHs (Guerrini et al., 2001), has been applied for γ-HDO samples to estimate their sulfation pattern. The percentage of substitution of glucosamine and uronic acid residues of four γ-HDO preparations are reported in Table 3, in comparison with the average values obtained from 10

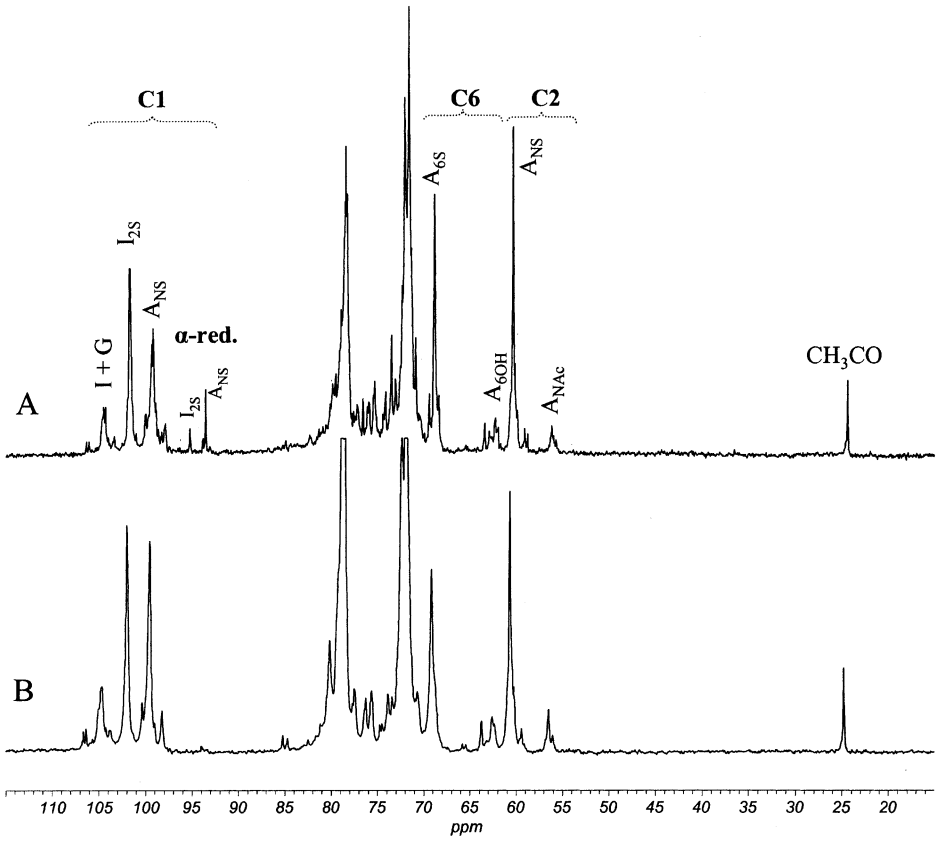

Fig. 2. ^{13}C NMR spectra obtained at 100 MHz of typical γ-HDO (A) and UFH (B).

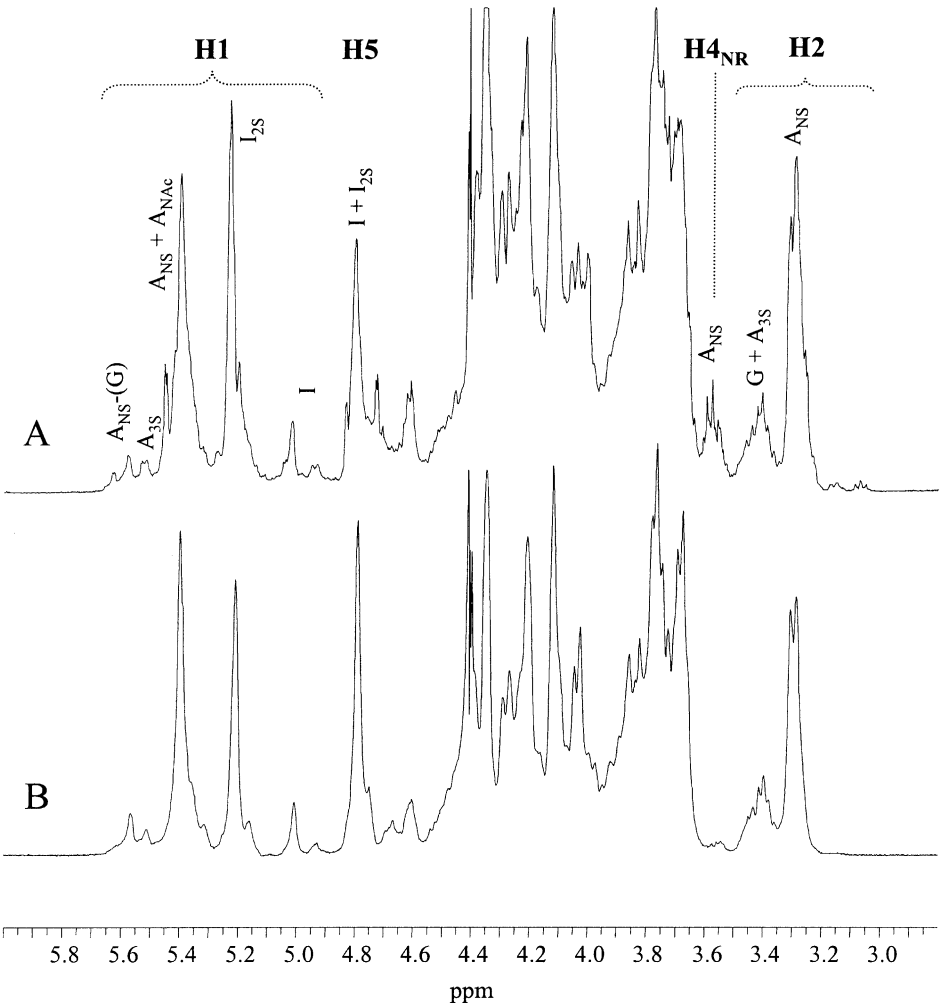

Fig. 3. ^{1}H NMR obtained at 500 MHz of typical γ-HDO (A) and UFH (B).

preparations of unfractionated pig mucosal heparin. The four different γ-HDO samples exhibited very similar sulfation patterns. Their average compositional analysis is similar to that of UFHs, apart from a significant decrease (about 13%) in depolymerized products of glucuronic acid residues. To verify whether this loss of G was due to a selective γ-ray-induced degradation or to the removal of the smallest undersulfated sequences by gel permeation chromatography, the ^{1}H and ^{13}C NMR spectra of the total γ-irradiated heparin mixture, before fractionation, were analysed (data not shown). The sulfation pattern of these samples was similar to that of γ-HDO fractions, with a comparable decrease of glucuronic acid (about 15%) with respect to UFHs.

A single preparation was studied in more detail with the aim of studying the effect of repeated γ-irradiation on

Table 3
Percent substitution of glucosamine and uronic acid residues of four γ-HDO preparations, obtained by a single γ-ray treatment of different UFHs

Sample	A_{NS}–I	A_{NS}–G	A_{NAc}	$A_{N,3,6S}$	A_{6S}[a]	I_{2S}	I_{2OH}	G
γ-HDO-a	69	8	16	6	81	68 (5)[b]	11	21
γ-HDO-b	67	9	17	7	78	67 (4)[b]	10	23
γ-HDO-c	69	9	16	6	85	66 (3)[b]	10	24
γ-HDO-d	72	8	15	5	82	67 (4)[b]	10	23
γ-HDO[c]	69.2 ± 1.78	8.5 ± 0.5	16.0 ± 0.71	6.0 ± 0.83	81.5 ± 2.49	67.0 ± 0.71	10.2 ± 0.43	23.0 ± 1.09
UFHs[c]	69.7 ± 1.50	9.6 ± 0.49	15.1 ± 1.67	5.8 ± 0.49	82.5 ± 0.80	62.7 ± 3.16	10.8 ± 1.22	26.4 ± 2.96

[a] Values obtained by integration of ^{13}C NMR signals.
[b] Values between brackets indicate the percentage of reducing 2-*O*-sulfated iduronic acid residues, which amounts are included in I_{2S} percentage values.
[c] Average data and SD of the γ-HDO analysed in comparison with the average data and SD of 10 UFHs.

Table 4
Percent substitution of glucosamine and uronic acid residues of three γ-HDO obtained by additional depolymerizing steps as described in Section 2, in comparison with their parent heparin (UFH-a)

Sample	$A_{NS}-I$	$A_{NS}-G$	A_{NAc}	$A_{N,3,6S}$	A_{6S}[a]	I_{2S}	I_{2OH}	G
UFH-a	69	10	15	5	86	59	12	29
γ-HDO-a	69	8	16	6	81	67 (5)[b]	11	21
γ-HDO-a2	71	9	14	6	84	70 (5)[b]	11	19
γ-HDO-a3	73	9	11	6	90	75 (4)[b]	10	16

[a] Values obtained by integration of ^{13}C NMR signals.
[b] Values between brackets indicate the percentage of reducing 2-*O*-sulfated iduronic acid residues, which amounts are included in I_{2S} percentage values.

heparin structure. The longer heparin chains of γ-HDOa little affected by the first γ-ray treatment, were isolated by gel chromatography as fraction H, and submitted to a second controlled γ-irradiation. The second generation of γ-depolymerized heparin oligosaccharides was fractionated as above, producing fractions H2, γ-HDOa2 and L2. Fraction H2 was again subjected to a third course of irradiation/fractionation, producing fractions H3, γ-HDO-a3 and L3. Fractions γ-HDOa2 and HDOa3 were then quali/quantitatively analysed by ^{1}H and ^{13}C NMR spectroscopy and their sulfation pattern was compared, together with γ-HDOa, with parent UFHa. As data in Table 4 show, all the samples significantly differ with respect to parent

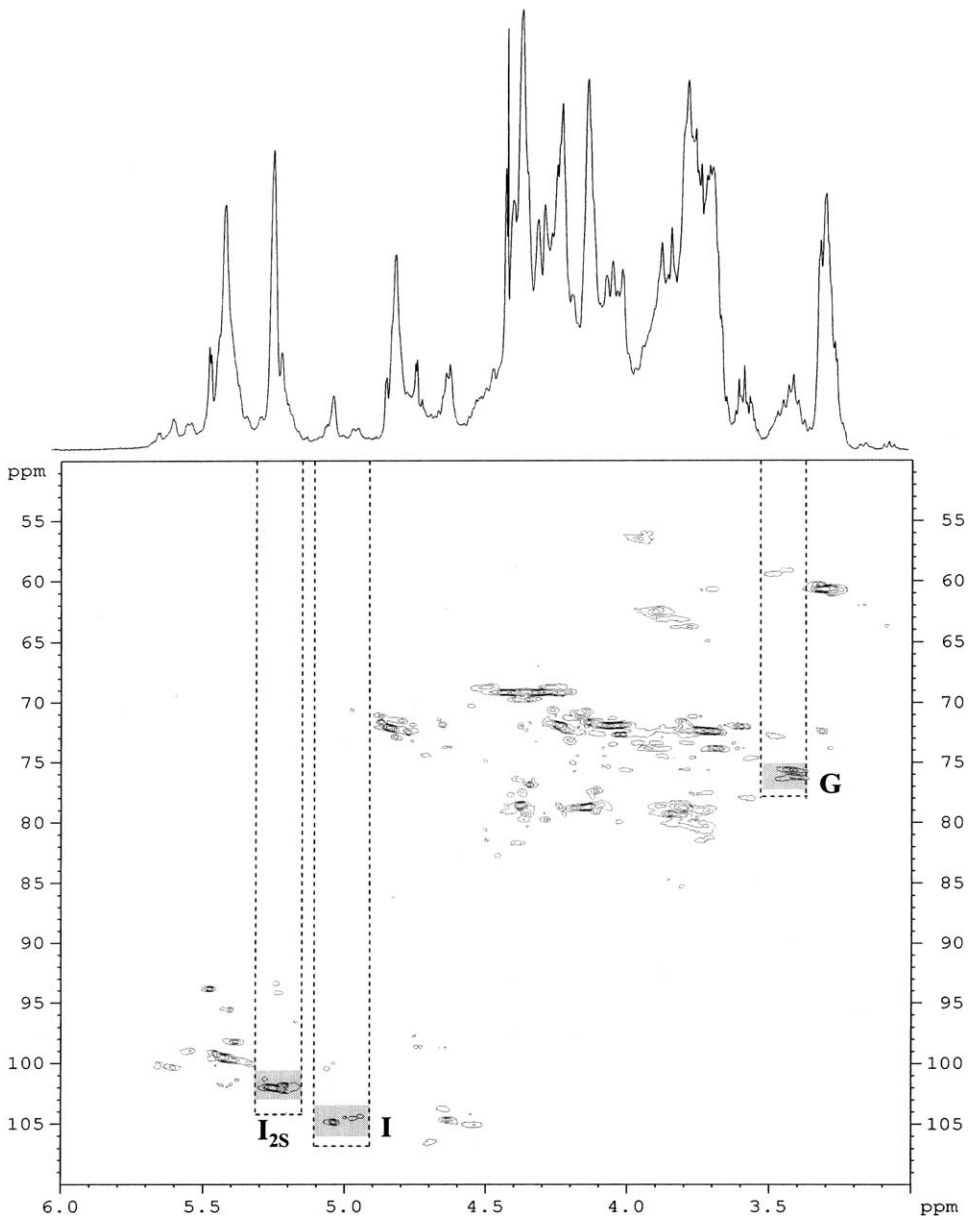

Fig. 4. Two-dimensional $^{1}H-^{13}C$ correlation spectrum (HSQC) of γ-HDO. The dashed bars indicate the regions used for the integration of the monodimensional ^{1}H spectrum. The grey areas indicate the specific signals used for the integration in the two-dimensional HSQC spectrum.

UFHa and from each other for the amount of glucuronic acid. G residue progressively decreased by increasing the number of γ-irradiation treatments, their relative percentages with respect to total uronic acids being in the range of 29% for UFHa up to 16% for γ-HDOa3 (Table 4). As regards other residues, γ-HDO-a and γ-HDOa2 did not show any significant variation. γ-HDOa3, the oligosaccharide fraction obtained by a triple γ-ray treatment, appears as the most homogeneous one, with significant increase of the content of A_{6S} as well as A_{NS} linked to total iduronic acid, and a reduction of the total content of unsulfated uronic acid and A_{NAc}. It is noteworthy that this over-irradiated fraction still shows an MW of 2200 Da, with a polydispersity similar to that of the other preparations. In the ^{13}C NMR spectra (not shown) of both γ-HDOa2 and γ-HDOa3, the signals associated with the LR disappear.

The analysis of all γ-HDO fractions by two-dimensional $^{1}H/^{13}C$ correlation spectrum (HSQC) revealed the presence of several minor signals absent in the corresponding spectra of parent UFHs. These signals are due to the high concentration of all possible reducing and non-reducing terminal residues and also to sequence effects, which assume great importance in short heparin chains. Some of these minor resonances overlapped the analytical signals used for quantitative analysis of major groups (indicated with dashed bars in Fig. 4), thus potentially affecting the calculation of sulfation pattern in γ-HDO samples. A few of these minor signals are known: for instance, resonances overlapping H1 of I_{2S} at about 5.21 are for both reducing H1α of A_{NAc} and reducing H1α of G (Chuang, McAllister, & Rabenstein, 2002). Other minor signals are unknown: for instance resonances at 5.1/100 and 3.46/72.9 ppm, overlapping H1 of I_{2OH} and H2 of G, respectively. To verify if the decrease of glucuronic acid content in γ-HDO following to γ-ray treatment actually occurred or was the resultant of summation of not proper resonances, the quantification of the specific heparin signals was carried out through the integration of their volume in the HSQC spectra, excluding interfering signals.

The volume integration of HSQC signals in 2D maps is currently used in relaxation studies for carbon T1 and T2 calculation (Kay, Nicholson, Delaglio, Bax, & Torchia, 1992). In this case the volume of each cross peak is measured as a function of the relaxation interval. In principle, quantitative comparison of cross peak volume of different atoms is possible only for atoms with comparable $^{1}J_{C-H}$ and relaxation time, as these parameters change in relation to the molecular environment (Yates et al., 2000). Since the objective was the verification of a decreasing trend of a heparin residue on a relative basis, and not the exact determination of its content, the integration of HSQC spectrum of a typical UFH was carried out by considering the same atoms of uronic acid residues as for monodimensional ^{1}H spectrum. Then, the two series of values (by HSQC and ^{1}H) were compared. Although the variability of the data, evaluated by analysing three times the same UFH, was slightly higher in the case of HSQC cross peak integration than for integration of monodimensional spectrum, the average results were comparable (unpublished data). HSQC cross peak integration was then performed also for γ-HDO samples by using signals indicated with grey labels in Fig. 4. In Table 5, the relative percentages of uronic acid residues for γ-HDO-c and UFH, calculated through both HSQC and monodimensional spectra, are compared. Regarding the quantification of reducing 2-*O*-sulfated iduronic acid residues of γ-HDOc, the correlation 5.38/95.6 was used in the case of HSQC, while in the case of monodimensional analysis, the carbon resonance at 95 ppm was currently used, as described in Section 2. Both for UFH and γ-HDOc, the two series of values were in good agreement, confirming that, despite the presence of minor interfering signals, also for γ-HDO samples the quantitative monodimensional NMR analysis was reliable.

MALDI mass spectrometric analysis was performed with the aim of identifying the main oligomeric components of γ-HDO preparations. For this purpose, γ-HDOc was fractionated by anion exchange chromatography in order to reduce the heterogeneity of sample in terms of number of charges. Column elution with a stepwise increasing salt concentration, at 0.4, 0.8, 1.0 and 2.0 M NaCl, divided γ-HDOc into four corresponding fractions: γ-HDOc-0.4, γ-HDOc-0.8, γ-HDOc-1.0 and γ-HDOc-2.0, with yields of 15, 61, 23 and 1%, respectively. After desalting by gel permeation chromatography, each fraction was analysed by MALDI. MALDI detection of these highly acidic oligosaccharide species is possible only as non-covalent 1:1 complexes with the synthetic peptide $(Arg-Gly)_{19}-Arg$, which acts as a shielding agent for the analyte, by replacing all the tightly attached alkali counterions. MWs, as determined from the difference between the mass value of the protonated peptide $[P + H]^{+}$ and the corresponding one for the oligosaccharide–peptide complex $[P + OS + H]^{+}$, allowed the heparin chains to be characterized in terms of number of monosaccharide units and sulfate (or acetyl) groups. Fig. 5 shows the MALDI spectrum and assignments of γ-HDOc-0.8 fraction, the most representative one of the total parent γ-HDOc, accounting for about 60%. The sample still consists of a very complex mixture of

Table 5
Percentage of uronic acid content for γ-HDOc and a typical UFH: comparison between values obtained by integration of monodimensional and HSQC spectra

Sample	I_{2S}		I_{2S}-red		I_{2OH}		G	
	^{1}H	HSQC	^{13}C	HSQC	^{1}H	HSQC	^{1}H	HSQC
UFH	58	61	–	–	11	9	31	30
γ-HDOc	63	65	3	3	10	10	24	22

I_{2S}-red indicates reducing 2-*O*-sulfated iduronic acid residues.

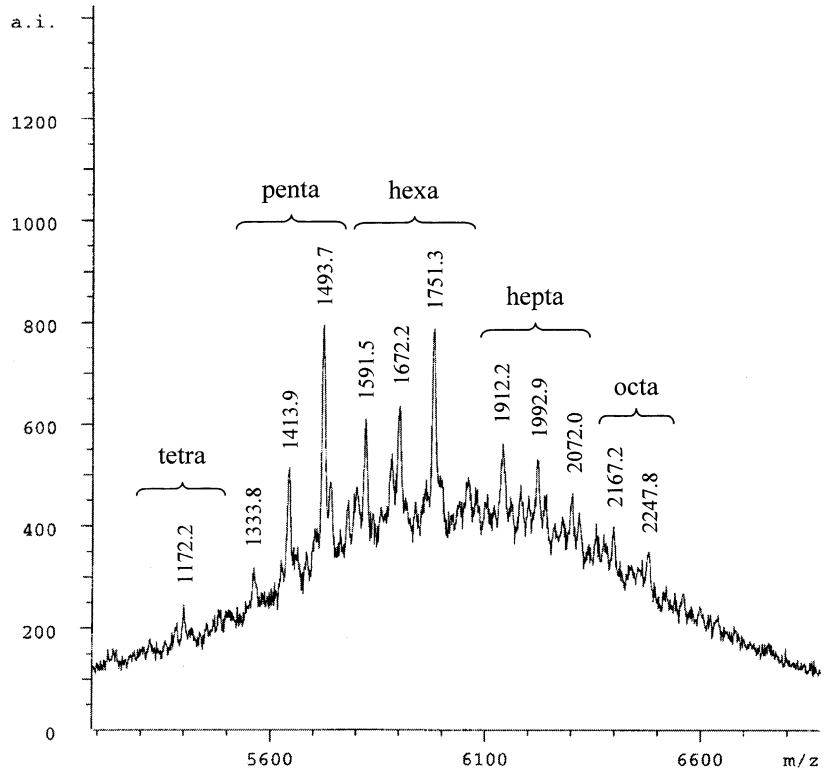

		calcd MW
$A_{NS,6S}$-I_{2S}-$A_{NS,6S}$-I_{2S}	tetrasaccharide 6 SO_3	1172.7
$A_{NS,6S}$-I/G-$A_{NS,6S}$-I_{2S}-A_{NS}	pentasaccharide 6SO_3	1334.0
$A_{NS,6S}$-I/G-$A_{NS,6S}$-I_{2S}-$A_{NS,6S}$	pentasaccharide 7 SO_3	1414.0
$A_{NS,6S}$-I_{2S}-$A_{NS,6S}$-I_{2S}-$A_{NS,6S}$	pentasaccharide 8 SO_3	1494.0
I_{2S} -$A_{NS,6S}$-I/G-$A_{NS,6S}$-I/G-$A_{NS,6S}$	hexasaccharide 7 SO_3	1590.1
I_{2S}-$A_{NS,6S}$-I/G-$A_{NS,6S}$-I_{2S}-$A_{NS,6S}$	hexasaccharide 8 SO_3	1670.1
I_{2S}-$A_{NS,6S}$-I_{2S}-$A_{NS,6S}$-I_{2S}-$A_{NS,6S}$	hexasaccharide 9 SO_3	1750.5
$A_{NS,6S}$-I/G-$A_{NS,6S}$-I_{2S}-$A_{NS,6S}$-I/G-$A_{NS,6S}$	heptasaccharide 9 SO_3	1911.1
$A_{NS,6S}$-I/G-$A_{NS,6S}$-I_{2S}-$A_{NS,6S}$-I_{2S}-$A_{NS,6S}$	heptasaccharide 10 SO_3	1991.1
$A_{NS,6S}$-I_{2S}-$A_{NS,6S}$-I_{2S}-$A_{NS,6S}$-I_{2S}-$A_{NS,6S}$	heptasaccharide 11 SO_3	2071.1
$A_{NS,6S}$-I/G-$A_{NS,6S}$-I_{2S}-$A_{NS,6S}$-I/G-$A_{NS,6S}$-I_{2S}	octasaccharide 10 SO_3	2167.2
$A_{NS,6S}$-I/G-$A_{NS,6S}$-I_{2S}-$A_{NS,6S}$-I_{2S}-$A_{NS,6S}$-I_{2S}	octasaccharide 11 SO_3	2247.2

Fig. 5. MALDI mass spectrum and assignments of γ-HDOc-0.8 fraction, with corresponding compatible structures and calculated MWs.

oligomers, ranging from tetra (1172.7) to octasaccharides (2248.0). Several separate peaks emerge, due to the major oligosaccharidic components. The corresponding compatible structures and calculated molecular mass values are also indicated in the figure. The MWs, obtained after subtracting the MW of the peptide, are in excellent agreement with the theoretical masses calculated for the different oligosaccharides. The proposed structures are also compatible with ^{1}H and ^{13}C NMR spectra of γ-HDOc-0.8 fraction (not shown).

4. Discussion

High energy irradiation often induces degradation of polymers. In particular, the degradation of polysaccharides largely occurs via splitting of a glycosidic bond. Mechanisms of radical-induced scission of the glycosidic linkage were proposed on the basis of results obtained from the γ-radiolysis of cellobiose, used as a small model compound. Anomeric radical resulted in the scission of the two sugar units. Nevertheless, both high energies involved and

the generation in water of the high reactive and unselective $OH^{\cdot}$ radical explain why radicals were generated in all the positions of sugar rings. The same mechanisms can be involved in the depolymerization of heparin (see Fig. 1). Different radicals were unselectively generated. Primary intermediate radicals are transformed by hydrolysis, rearrangements, water or carbon monoxide elimination and all possible combination thereof. When radicals disappeared by disproportionation reactions, unsaturations were introduced (Giese, 1986).

During the γ-radiolysis of heparin, anomeric radicals in undersulfated regions mainly caused depolymerization (Table 2) (Von Sonntag et al., 1976). At the same time, the parallel complex radical pathways probably introduced unsaturated structures and chromophores responsible for unwanted anomalous absorbances in UV/visible region shown especially in the case of oligosaccharides derived from heparin treated with high doses of γ rays. An important goal should be to divert radical pathways towards depolymerization, limiting side-reactions and thus reducing the absorbancies.

Table 1 reports results of irradiation experiments run alone or in the presence of small molecules containing weak C–H bonds, as shown by the reported BDE. These molecules can influence depolymerization in two different ways: (i) by generating radicals from their weak C–H in competition with radicals generation on heparin; (ii) by trapping as hydrogen donor scavengers part of OH radicals and heparin intermediate radical adducts. Whatever roles they play, they are transformed anyway into volatile organic compounds which can easily be eliminated from the reaction mixtures. As far as we know, no data are available about BDE of C–H of polysaccharides; nevertheless they are probably similar to O–C–H of alcohols and ethers, except for the anomeric position. The presence of two oxygens makes it easier to generate anomeric radicals than non-anomeric radicals. Furthermore, anomeric radicals present a certain degree of stability that contributes to their generation. As shown by Table 1, depolymerization occurred also in the presence of all the selected molecules. Alcohols, THF and formic acid seem to play a different role than acetic acid and malonates. The latter two limited somewhat depolymerization and did not reduce the absorbance. Formic acid reduced the absorbance but at the same time limited the depolymerization. Alcohols and THF were successfully employed: the MW was only slightly modified, while absorbance values decreased. The important goal obtained with them is to make the γ-ray depolymerization cleaner and more controlled. Due to their structures, such small molecules did not compete with anomeric radicals generation, while successfully competing with the generation of non-anomeric radicals. So the more important radicals for the depolymerization were mainly generated, the anomeric ones, and the other radicals that made the process unselective were limited. Alcohols and THF probably trapped heparin intermediate radicals, thus limiting both the disproportion and the formation of unsaturations and chromophores. In conclusion, alcohols and THF allowed depolymerization to occur while contributing to the maintenance of unchanged internal structures.

In the present study, pig mucosal heparin was depolymerized by controlled irradiation with γ-rays in order to obtain oligosaccharide fragments with size ranging from tetra to decasaccharides. The four HDO preparations obtained from different UFHs, isolated as intermediate fractions from the gel chromatographic profile of the total depolymerized mixtures, were characterized in terms of molecular weight, anti-Xa activity and structural features. All samples exhibited very similar characteristics, thus proving good reproducibility of the depolymerizing procedure, independent of the parent heparin.

Together with an average molecular weight of about 2200 Da and a low degree of polydispersity, γ-HDO still exhibits appreciable anti-Xa potencies. Such potency is a measure of the ability of heparin sequences to inhibit the Xa factor by interacting with AT and suggests that in γ-HDO preparations the pentasaccharidic sequence (active site for AT) is preserved to quite a good extent.

A qualitative comparison between ^{1}H and ^{13}C NMR spectra of a typical γ-HDO preparation and those of its parent UFH (Figs. 2 and 3) displays a good degree of structural similarity, the main differences relate only to minor peaks. For instance, in the carbon spectrum new signals correspond to reducing I_{2S} and $A_{N,6S}$ residues, while in the hydrogen spectrum, the H4 signal of the non-reducing *N*-sulfated glucosamine residue markedly increase.

The combined quantitative ^{1}H and ^{13}C NMR analysis of major as well as some minor but biologically important structural features, provided the characterization of the sulfation pattern at the different positions of the uronic acid and glucosamine residues. As indicated by data shown in Table 2, a high compositional homogeneity of the four γ-HDO preparations is evident. By comparing the average values for γ-HDO and the average values obtained for 10 pig mucosal UFHs, including parent UFHs, a decrease of the glucuronic acid relative content appears, while the content of all other residues was by and large unmodified. Quantitative NMR evaluation revealed that a comparable decrease of glucuronic acid was also detected from the spectra of the γ-irradiated heparin mixture before the gel permeation step. Previous results indicated that γ-irradiation preferably acts on undersulfated heparin regions, generating short heparin sequences (Bisio et al., 2001). Nevertheless the present results suggest that the loss of G is attributable more to its degradation by γ-rays than to its chromatographic removal as a component of minor oligosaccharidic fragments.

With increasing fragmentation of heparin chains, also the complexity of ^{13}C and especially of ^{1}H NMR spectra of depolymerized samples increases, both because of

the numerous signals of reducing and non-reducing termini, and also the increasing influence of sequence effects.

The two-dimensional proton–carbon correlation spectra (HSQC) of γ-HDO samples show the presence of new minor resonances, with respect to UFH, a few of which, in monodimensional ^{1}H spectrum overlap some analytical signals chosen for integration, affecting their quantification. For instance, very weak signals at about 94–93 and 5.2 ppm, due to reducing end residues of G and A_{NAc} are observed. To determine if, despite the presence of possible interferences, the observed decrease of glucuronic acid content is apparent or real, the quantification of analytical heparin signals in HDO samples was performed also by integrating their volumes in the HSQC spectrum, thus avoiding interfering signals. The same procedure, i.e. integration of both areas and volumes of specific signals in mono and bi-dimensional spectra, respectively, was also applied to UFH. Then, the percentage of glucuronic acid obtained with the two procedures was compared. While, as expected, similar values were obtained for UFHs, for γ-HDO some discrepancies were observed. The percentage of glucuronic acid calculated via HSQC was somewhat lower with respect to ^{1}H NMR. This result, however, confirms that the glucuronic acid content actually decreases in γ-HDOs with respect to parent UFHs. Thus, despite the limitation of the combined quantitative ^{1}H and ^{13}C NMR approach for the characterization of depolymerized heparins due to the presence of possible interfering signals, this method can also provide a sufficiently good estimation of the sulfation pattern for γ-HDO samples.

In order to verify the possible selectivity of radical depolymerization, the heparin chains that were not affected, or not affected significantly, by γ-ray depolymerization, were isolated by gel chromatography as fraction H during the preparation of γ-HDOa (see Section 2), and were recovered and submitted to a second controlled γ-irradiation process. The second generation of γ-depolymerized heparin oligosaccharides was fractionated as above, producing fractions H2, γ-HDOa2 and L2. Again fraction H2 was subjected to a second course of irradiation and fractionation, producing fractions H3, γ-HDOa3 and L3.

Both γ-HDOa2 and γ-HDOa3 exhibited molecular weight polydispersity and anti-Xa potency values comparable with the corresponding values of all the other γ-HDO fractions subjected only to a single γ-ray treatment. Their sulfation pattern, evaluated by ^{1}H and ^{13}C NMR, compared with those of γ-HDOa and of the parent UFHa, reveals some significant changes. The glucuronic acid content progressively decreases from γ-HDOa to γ-HDOa2 and γ-HDOa3. In the latter a reduction of the *N*-acetyl glucosamine content also appears, though quantitatively less important than the G decrease: their percentage values of A_{NAc} decreases with respect to UFHa by about 30 and 50%, respectively. Apart from the expected increase in the relative percentage of I_{2S} and A_{NS}, the content of all the other residues remained substantially unchanged.

It is worth underlining that both after single and additional γ-ray treatments, the percentage of *N*,3,6-sulfated glucosamine, marker of the heparin active site for AT, did not change with respect to UFH. This result, together with the data of anti-Xa activity evaluation, indicates that in γ-HDO preparation the integrity of the active site for AT is maintained to a relatively high extent.

These results, confirm that controlled γ-irradiation in the presence of isopropanol cleaves glycosidic linkage preferentially at the level of the glucuronic acid residues particularly in the undersulfated heparin region, where the presence of $G-A_{NAc}$ disaccharidic units prevails. The shorter heparin sequences generated by depolymerization are lost through gel chromatography on Sephadex G-50. Accordingly, as data in Table 4 show, this depolymerizing method allows the isolation of heparin oligosaccharides enriched in highly sulfated sequences.

This finding is in agreement with the interpretation of MALDI spectrum (Fig. 5) of a γ-HDO fraction, isolated by anion exchange chromatography of a γ-HDOc and accounting for about 60% of it. The proposed structures, ranging from tetra to decasaccharides, are in very good agreement with the molecular mass values of the major oligosaccharidic components. The deduced compositions can correspond to more than one sequence due to the number of possible dimeric combinations. They are characterized by a high degree of sulfation. The strongest MALDI peaks correspond to penta- and hexasaccharides constituted by I_{2S} and $A_{NS,6S}$ residues as in the major product of heparin biosynthesis. An interesting finding emerging from the MALDI spectrum is that γ-irradiation, in contrast with most of the other depolymerizing methods (Linhardt & Gunay, 1999), can generate oligosaccharide sequences composed by both even and uneven number of monosaccharidic units. Moreover, the most represented sequences among the uneven oligosaccharides start and end with *N*-sulfated glucosamine units. This observation also agrees with the ^{13}C and ^{1}H NMR spectra of γ-HDO preparations, where respectively appear that, in the region of reducing anomeric carbons, the most prominent resonance was that of A_{NS} and the H4 of the non-reducing A_{NS} residue markedly increased with respect to parent UFH.

These data suggest that controlled γ-irradiation in the presence of isopropanol, cleave (1 → 4) glycosidic linkage between non-sulphated uronic acid, mainly G residue, and glucosamine residues. Only a small amount of G (of the order of 2% of the total amount of uronic acids) is recovered as a reducing end, this means that the large part of the corresponding G ring radical residue is lost. It can, in some way, rearrange to open structures as shown in Fig. 1. However, no spectroscopic evidence of such open structures was found. The most probable explanation of this absence is that they are lost as volatile fragments during the oxidative bleaching treatment that exposes new reducing glucosamine residues. This fact is in agreement with the presence of both odd and even number of monomers in the oligomeric chains.

Acknowledgements

The authors would like to thank Prof. B. Casu for useful discussion.

References

Bisio, A., De Ambrosi, L., Gonella, S., Guerrini, M., Guglieri, S., Maggia, G., & Torri, G. (2001). Preserving the original heparin structure of a novel low molecular weight heparin by γ-irradiation. *Arzneimittel-Forschung/Drug Research*, *51*, 806–812.

Bitter, T., & Muir, H. M. (1962). Quantitative determination of uronic acids with *m*-hydroxydiphenyl. *Analytical Biochemistry*, *4*, 330.

Capila, I., & Linhardt, R. J. (2002). Heparin–protein interaction. *Angewandte Chemie*, *41*, 390–412.

Casu, B. (1985). Structure in biological activities of heparin. *Advances in Carbohydrate Chemistry and Biochemistry*, *43*, 51–134.

Casu, B., & Lindahl, U. (2001). Structure and biological interactions of heparin and heparan sulfate. *Advances in Carbohydrate Chemistry and Biochemistry*, *57*, 159–208.

Casu, B., & Torri, G. (1999). Structural characterization of low molecular weight heparins. *Seminars in Thrombosis and Hemostasis*, *25*(3), 17–25.

Chuang, W. L., McAllister, H., & Rabenstein, D. (2002). Hexasaccharides from the istamine-modified depolymerization of porcine intestinal mucosal heparin. *Carbohydrate Research*, *337*, 935–945.

Dietrich, C. P., Tresariol, I. L., Toma, L., Moraes, C. T., Porcionatto, M. A., Oliveira, F. W., & Nader, H. B. (1998). Structure of heparan sulfate: Identification of variable and constant oligosaccharide domains in eight heparan sulfates of different origin. *Cellular and Molecular Biology*, *44*, 417–429.

Farmer, T. B., & Caprioli, R. M. (1998). Determination of protein–protein interactions by matrix-assisted laser desorption/ionization mass spectrometry. *Journal of Mass Spectrometry*, *33*, 697–704.

Gambarini, A. G., Miyamoto, C. A., Lima, G. A., Nader, H. B., & Dietrich, C. P. (1993). Mitogenic activity of acidic fibroblast growth factor is enhanced by highly sulfated oligosaccharides derived from heparin and heparan sulfate. *Molecular and Cellular Biochemistry*, *124*, 121–129.

George, C., El Rassy, H., & Chovelon, J. M. (2001). Reactivity of selected volatile organic compounds (VOCs) toward the sulfate radical (SO_4^{-}). *International Journal of Chemical Kinetics*, *33*, 539–547.

Giese, B. (1986). Basic principles. In J. E. Baldwin (Ed.), (*Vol. 5*) (pp. 4–35). *Radicals in organic syntheses: Formation of C–C bonds*, Oxford: Pergamon Press.

Gonella, S., De Ambrosi, L., & Vismara, E (2002). *European Patent* EP02 425142.3.

Guerrini, M., Bisio, A., & Torri, G. (2001). Combined quantitative ^{1}H and ^{13}C nuclear magnetic resonance spectroscopy for characterization of heparin preparations. *Seminars in Thrombosis and Hemostasis*, *27*, 473–482.

Kay, L. E., Nicholson, L. K., Delaglio, F., Bax, A., & Torchia, D. A. (1992). Pulse sequences for removal of the effects of cross correlation between dipolar and chemical-shift anisotropy relaxation mechanisms on the measurement of heteronuclear T_1 and T_2 values in proteins. *Journal of Magnetic Resonance*, *97*, 359–375.

Leveugle, B., Ding, W., Laurence, F., Dehouck, M. P., Scanameo, A., Cecchelli, R., & Fillit, H. (1998). Heparin oligosaccharides that pass the blood-brain barrier inhibit β-amyloid precursor protein secretion and heparin binding to β-amyloid peptide. *Journal of Neurochemistry*, *70*, 737–744.

Lindahl, U., Kusche-Gulberg, M., & Kjellen, L. (1998). Regulated diversity of heparan sulfate. *The Journal of Biological Chemistry*, *273*, 24979–24982.

Linhardt, J. R., & Gunay, N. S. (1999). Production and chemical processing of low molecular weight heparins. *Seminars in Thrombosis and Hemostasis*, *25*, 5–16.

Maccarana, M., Casu, B., & Lindahl, U. (1993). Minimal sequence in heparin/heparan sulfate required for binding of basic fibroblast growth factor. *The Journal of Biological Chemistry*, *268*, 23898–23905.

Moy, F. J., Safran, M., Seldon, A. P., Kitchen, D., Böhlen, P., Aviezer, D., Yayon, A., & Powers, R. (1997). Properly oriented heparin-decasaccharide-induced dimers are biologically active form of basic fibroblast growth factor. *Biochemistry*, *36*, 4782–4791.

Petitou, M., Imberty, A., Duchaussoy, P., Driguez, P. A., Ceccato, M. L., Gouvernec, F., Sizun, P., Hérault, J. P., Pérez, S., & Herbert, J. M. (2001). Experimental proof of the structure of a thrombin-inhibiting heparin molecule. *Chemistry—A European Journal*, *7*(4), 858–873.

Rose, M., Dudas, B., Cornelli, U., & Hanin, I. (2003). Protective effect of the heparin-derived oligosaccharide C3, on AF64A-induced cholinergic lesion in rats. *Neurobiology of Aging*, *24*, 481–490.

Sudhalter, J., Folkman, J., Svahn, C. M., Bergendal, K., & D'Amore, P. A. (1989). Importance of size, sulfation, and anticoagulant activity in the potentiation of acidic fibroblast growth factor by heparin. *Journal of Biological Chemistry*, *264*, 6892–6897.

Teien, A. N., & Lie, M. (1977). Evaluation of an amidolytic heparin assay method: Increased sensitivity by adding purified antithrombin III. *Thrombosis Research*, *10*, 399–410.

Venkataraman, G., Shriver, Z., Davis, J. C., & Sasisekharan, R. (1999a). Fibroblast growth factor 1 and 2 are distinct in oligomerization in the presence of heparin-like glycosaminoglycans. *Proceedings of the National Academy of Sciences, USA*, *96*, 1892–1897.

Venkataraman, G., Shriver, Z., Raman, R., & Sasisekharan, R. (1999b). Sequencing complex polysaccharides. *Science*, *286*, 537–542.

Von Sonntag, C., Dizdaroglu, M., & Schulte-Frohlinde, D. (1976). Radiation chemistry of carbohydrates, VIII*. γ-Radiolysis of cellobiose in N_2O-saturated aqueous solution. Part II. Quantitative measurements. Mechanism of the radical-induced scission of the glycosidic linkage. *Zeitschrift fuer Naturforschung, Teil B: Anorganische Chemie, Organische Chemie*, *31B*, 857–864.

Walzer, M., Lorens, S., Hejna, M., Fareed, J., Hanin, I., Cornelli, U., & Lee, J. M. (2002). Low molecular weight glycosaminoglycan blockade of β-amyloid induced neuropathology. *European Journal of Pharmacology*, *445*, 211–220.

Yates, E. A., Santini, F., De Cristofano, B., Payre, N., Cosentino, C., Guerrini, M., & Hricovini, M. (2000). Effect of substitution pattern on ^{1}H, ^{13}C NMR chemical shift and $^{1}J_{CH}$ coupling constant in heparin derivatives. *Carbohydrate Research*, *329*, 239–247.